

## On the human sensorimotor-cortex beta rhythm: Sources and modeling

O. Jensen,<sup>a,b,\*</sup> P. Goel,<sup>c</sup> N. Kopell,<sup>d</sup> M. Pohja,<sup>a</sup> R. Hari,<sup>a,e</sup> and B. Ermentrout<sup>f</sup>

<sup>a</sup>Brain Research Unit, Low Temperature Laboratory, Helsinki University of Technology, Finland

<sup>b</sup>F.C. Donders Centre for Cognitive Neuroimaging, Radboud University Nijmegen, NL-6500 HB Nijmegen, The Netherlands

<sup>c</sup>Mathematical Biosciences Institute, Ohio State University, OH 43210, USA

<sup>d</sup>Department of Mathematics, Boston University, MA 02215, USA

<sup>e</sup>Department of Clinical Neurophysiology, Helsinki University Central Hospital, 00270 Helsinki, Finland

<sup>f</sup>Department of Mathematics, University of Pittsburgh, PA 15260, USA

Received 24 March 2004; revised 24 January 2005; accepted 9 February 2005  
Available online 7 April 2005

Cortical oscillations in the beta band (13–35 Hz) are known to be modulated by the GABAergic agonist benzodiazepine. To investigate the mechanisms generating the  $\approx 20$ -Hz oscillations in the human cortex, we administered benzodiazepines to healthy adults and monitored cortical oscillatory activity by means of magnetoencephalography. Benzodiazepine increased the power and decreased the frequency of beta oscillations over rolandic areas. Minimum current estimates indicated the effect to take place around the hand area of the primary sensorimotor cortex. Given that previous research has identified sources of the beta rhythm in the motor cortex, our results suggest that these same motor-cortex beta sources are modulated by benzodiazepine. To explore the mechanisms underlying the increase in beta power with GABAergic inhibition, we simulated a conductance-based neuronal network comprising excitatory and inhibitory neurons. The model accounts for the increase in the beta power, the widening of the spectral peak, and the slowing down of the rhythms with benzodiazepines, implemented as an increase in GABAergic conductance. We found that an increase in IPSCs onto inhibitory neurons was more important for generating neuronal synchronization in the beta band than an increase in IPSCs onto excitatory pyramidal cells.

© 2005 Elsevier Inc. All rights reserved.

**Keywords:** Beta rhythm; Sensorimotor cortex; Electroencephalographic; Magnetoencephalographic

### Introduction

Oscillatory activity of the human cerebral cortex, readily monitored by electroencephalographic (EEG) and magnetoence-

phalographic (MEG) recordings, comprises several prominent frequency bands. The best known is the  $\approx 10$  Hz parieto-occipital “alpha” rhythm that reacts strongly to opening/closing of the eyes. The rolandic mu-rhythm is observed as spontaneous activity in healthy subjects over sensorimotor areas and has a 10-Hz and 20-Hz components that have different sources in the primary somatosensory and the motor cortex, respectively, (see Hari and Salmelin, 1997 for a review). The 20-Hz rhythm is modulated during various motor and cognitive tasks (Farmer, 1998; Hari and Salmelin, 1997). Moreover, a part of the 20-Hz motor-cortex oscillations are coherent with simultaneously recorded surface electromyogram during isometric contraction (Conway et al., 1995; Salenius et al., 1997) and have been suggested to be related to re-calibration after movements (Kilner et al., 1999). Patients with progressive myoclonus epilepsy and chronic pain display abnormal reactivity of the motor-cortex beta-range activity (Juottonen et al., 2002; Silen et al., 2000), suggesting reduced intracortical inhibition.

In clinical EEG records, rhythmic beta oscillations are observed in frontal scalp electrodes in subjects who have taken benzodiazepine-type drugs (Wanquier, 1998). Interestingly, Baker and Baker (2003) reported that cortico-muscle coherence in the beta range decreased after the application of benzodiazepines. Our experimental aim was to investigate whether benzodiazepine would modify the motor-cortex 20-Hz oscillations measured by MEG in healthy subjects. Furthermore, we were interested in finding out whether we could identify the generation site(s) of the beta-range rhythms after benzodiazepine administration. Preliminary results on this subject (Jensen et al., 2002) prompted the current study.

The primary effect of benzodiazepines is an increase in the conductance of  $GAB_A$ -mediated currents. It is not intuitive how the resulting increase in inhibition could increase the power of a rhythm and why that increase would be in the beta band. We use suggestions from in vitro research and computational modeling to help to provide an answer. The human beta oscillations appear to have many features in common with gamma band oscillations

\* Corresponding author. F.C. Donders Center for Cognitive Neuroimaging, P.O. Box 9101, NL-6500 HB Nijmegen, The Netherlands. Fax: +31 24 36 10989.

E-mail address: ole.jensen@fcdonders.ru.nl (O. Jensen).

Available online on ScienceDirect (www.sciencedirect.com).

(30–80 Hz) observed in various animal preparations. Gamma oscillations have been modeled *in vitro* in the hippocampus (Towers et al., 2002; Traub et al., 1996; Whittington et al., 1995, 1997a). In those preparations, the fast-spiking interneurons are important for the gamma frequency oscillations. Bacci et al. (2003) and Faulkner et al. (1999) recently showed that these are the interneurons affected by benzodiazepine-like agonists. Interestingly, Shimono et al. (2000) showed that cholinergically induced beta oscillations in hippocampal rat slice increased in power and decreased in frequency by benzodiazepine.

The computational network model we offer hypothesizes that the human beta oscillations in the sensorimotor cortex are an analogue of the gamma oscillations studied in rats. Networks of inhibitory interneurons have shown to be crucially involved in generating the gamma rhythm (Towers et al., 2002; Traub et al., 1996; Whittington et al., 1995, 1997a). The main motivation for hypothesizing this analogy is the sensitivity in frequency and power of these rhythms to GABAergic agonists, suggesting a strong role to be played by the interneuronal network. The frequencies of the rhythms are affected by the size and decay time of the  $GAB_A$  conductance and the drive to both excitatory and inhibitory neurons. We show a parameter range in which all the behavior of the power spectrum described in the experimental findings is replicated. Specifically, modeling the effects of benzodiazepine as an increase in the strength of the  $GAB_A$  conductance, we show that this can increase the power in the beta frequency range, lower the frequency and broaden the range in which there is large power. We show that the major effects come about from an increase in inhibitory current to the inhibitory interneurons; instead, increase in inhibitory currents to the excitatory pyramidal cells does not increase the beta power.

## Materials and methods

### Subjects

Magnetoencephalographic (MEG) signals were recorded from eight healthy subjects (ages 26–35 years; 3 males; 5 females) with no history of neurological disorders. Informed consent was obtained from each subject after full explanation of the study. The work had a prior approval by the ethics committee of the Helsinki Uusimaa Hospital District.

### Procedure

The subjects were seated in a relaxed position under the MEG helmet. They were instructed to keep their eyes closed and relax without falling asleep while 3 min of ongoing MEG signals were recorded. Following this control condition, about 80  $\mu\text{g}/\text{kg}$ , i.e. 4–7.5 mg benzodiazepine (Diapam<sup>®</sup>) was administered orally. Following a 1-h break, the MEG measurement was repeated.

### Data acquisition

MEG signals were recorded with a helmet-shaped 306-channel detector array (Vectorview<sup>™</sup>, Neuromag Ltd, Helsinki, Finland). This system has 102 triple-sensor elements distributed over the scalp, each element comprising two planar gradiometers and one magnetometer. Typically, the local neuronal sources of the signals are situated directly below those planar gradiometers that detect the

strongest signals. To measure the head position with respect to the sensors, four coils were placed on the scalp, and their relative positions with respect to anatomical landmarks on the head were determined with a 3-D digitizer. After the subjects were seated under the MEG helmet, the positions of the coils were determined by measuring the magnetic signals produced by currents passed through the coils. Magnetic resonance images (MRIs) were obtained with a 1.5 T Siemens Magnetom scanner and were aligned to the MEG coordinate system according to anatomical landmarks. The ongoing MEG signals were bandpass filtered from 0.1 to 100 Hz, digitized at 300 Hz and stored for off-line analysis.

### Data analysis

Power spectra of the neuromagnetic signals were calculated for each sensor before and after benzodiazepine application according to Welch's method (Press et al., 1997) (Hanning window, 50% overlapping 2048-points window). The dominant oscillatory signals were identified and characterized from the spectra. For source determination, the peak frequency in the beta band was first identified for each subject and at these frequencies minimum current estimates were calculated (Uutela et al., 1999). Applying a sliding time window approach, this method allows us to calculate the current distribution in the frequency domain. For each time window, the minimum current estimate is calculated for the frequency of interest. Subsequently, the absolute contributions of the real and imaginary parts of the current estimates are averaged (Jensen and Vanni, 2002). In several subjects, the sources of the beta-range oscillations were then mapped onto the subject's own MRI (Uutela et al., 1999).

### Modeling

The network consisted of 64 excitatory pyramidal neurons (e-cells) and 16 inhibitory interneurons (i-cells) connected all-to-all but with a weak e–e coupling. This type of network model allows us explore the physiological mechanisms and dynamics producing the beta oscillations. The model is constrained by the kinetics of membrane and synaptic currents. The i-cells were modeled with equations

$$C \frac{dV_i}{dt} = -g_L(V_i - V_L) - g_K n^4 (V_i - V_K) - g_{Na} m^3 h (V_i - V_{Na}) - I_{syn,i} + I_0$$

and the e-cells by equations of the form:

$$C \frac{dV_e}{dt} = -g_L(V_e - V_L) - g_K n^4 (V_e - V_K) - g_{Na} m^3 h (V_e - V_{Na}) - g_{AHP} w (V_e - V_K) - I_{syn,e} + I_0$$

Both types of cells have a leak (L), a transient sodium (Na) and a delayed rectifier potassium (K) current. The e-cells have an additional after-depolarizing potential (AHP) resulting in a slow outward potassium current. Parameters and functional forms of the equations are taken from Traub and Miles (1991).

The gating variables  $m$ ,  $h$ ,  $n$  satisfy equations of the form:

$$\frac{dx}{dt} = a_x(V)(1-x) - b_x(V)x$$

for  $x = m, h, n$  where

$$a_m(V) = 0.32(54 + V)/(1 - \exp[-(V + 54)/4])$$

$$b_m(V) = 0.28(V + 27)/(\exp[(V + 27)/5] - 1)$$

$$a_h(V) = 0.128 \exp(-(50 + V)/18)$$

$$b_h(V) = 4/(1 + \exp[-(V + 27)/5])$$

$$a_n(V) = 0.032(V + 52)/(1 - \exp[-(V + 52)/5])$$

$$b_n(V) = 0.5 \exp[-(57 + V)/40].$$

The gating variable  $w$  satisfies

$$\frac{dw}{dt} = (w_\infty(V) - w)\tau_w(V)$$

where

$$w_\infty(V) = 1/(1 + \exp[-(V + 35)/10])$$

$$\tau_w(V) = 400/(3.3 \exp[(V + 35)/20] + \exp[-(V + 35)/20]).$$

The maximal conductances were  $g_{Na} = 100$  mS/cm<sup>2</sup>,  $g_K = 80$  mS/cm<sup>2</sup>,  $g_L = 0.1$  mS/cm<sup>2</sup>, and  $g_{AHP} = 0.3$  mS/cm<sup>2</sup>. Reversal potentials were  $V_L = -67$  mV,  $V_K = -100$  mV, and  $V_{Na} = 50$  mV. The capacitances for e- and i-cells were 1  $\mu$ F/cm<sup>2</sup>. Parameters for both the e-cells and i-cells were the same; the only differences are in the synaptic currents and the driving currents,  $I_0$ . Even though these models initially were developed for hippocampal pyramidal and inhibitory neurons, they are sufficiently general to be applied to neocortical neurons as well. Since the axons and dendrites of the neurons are not modeled specifically, the layer-specific differences between hippocampal and neocortical neurons are not taken into account.

The synaptic currents were of the form:

$$I_{syn,x} = g_{ix}s_{i,tot}(V_x - V_{in}) + g_{ex}s_{e,tot}(V_x - V_{ex})$$

for  $\alpha = e, i$ . Reversal potentials were  $V_{ex} = 0$  mV and  $V_{in} = -80$  mV. The synaptic gates are described by:

$$s_{\alpha,tot} = \frac{1}{N_{\alpha-cells}} \sum s_{\alpha}$$

$$\frac{ds_{\alpha}}{dt} = a_{\alpha}(1 + \tanh(V_{\alpha/4}))(1 - s_{\alpha}) - s_{\alpha}/\tau_{\alpha}$$

where  $a_e = 20$ /ms,  $a_i = 1$ /ms,  $\tau_e = 2.4$  ms, and  $\tau_i = 12$  ms. The inhibitory GABA<sub>A</sub> conductances,  $g_{ie}$ ,  $g_{ii}$  varied respectively from 5 to 7 mS/cm<sup>2</sup> and 10 to 20 mS/cm<sup>2</sup>. The exact values are given in the text. The excitatory conductances were  $g_{ee} = 0.01$  mS/cm<sup>2</sup> and  $g_{ei} = 0.05$  mS/cm<sup>2</sup>. Note that the small values of the excitatory synaptic conductances can reflect sparseness in connectivity as well as a small absolute value of the AMPA receptor conductivity.

Noise determined by Gaussian distribution was added to the voltages at each integration step. The magnitude for the noise was respectively 1.0 and 0.5 mV<sup>2</sup>/ms for the e- and i-cells. The equations were integrated using Euler's method with a time step of 0.025 ms. Smaller values yielded no qualitatively different results. The power spectra are computed using the total excitatory synaptic currents to the e-cells:

$$EPSC_{tot} = \sum_{i-cells} g_{ee}s_{e,tot}(V_{ex} - V_e) \quad (1)$$

The value of this entity is primarily determined by the spiking of the e-cells. The field measured by the MEG is thought to be a consequence of post-synaptic currents (PSCs) flowing in pyramidal cells (Hämäläinen et al., 1993) and weighted toward the EPSCs. Such currents in the dendrites do not necessarily cause spiking at the e-cell somata. We model this by making the e–e connections, which in our one-compartment model do affect spiking, very small. We note that the e–e connections are not necessary for the rhythms we simulate and can disrupt those rhythms if the recurrent excitation is too large.

Heterogeneity was introduced to the network by providing variations in the input currents ( $I_0$ ) in the range from 0.6 to 2.0  $\mu$ A/cm<sup>2</sup> to the e-cells and from 1 to 1.1  $\mu$ A/cm<sup>2</sup> to the i-cells. These currents were chosen so that, in the absence of the inhibitory input, few of the cells fired. Cells that did fire, fired at frequencies lower than the beta range. During rest, neuromodulators such as ACh are lower than in active states. Low ACh is known to increase the AHP-currents ( $I_{AHP}$ ). This motivates the choice of relatively strong AHP-currents ( $I_{AHP}$ ).

## Results

### Experiments

Fig. 1 shows power spectra for subject S2 before (pre-BNZ) and after (post-BNZ) benzodiazepine administration, respectively.

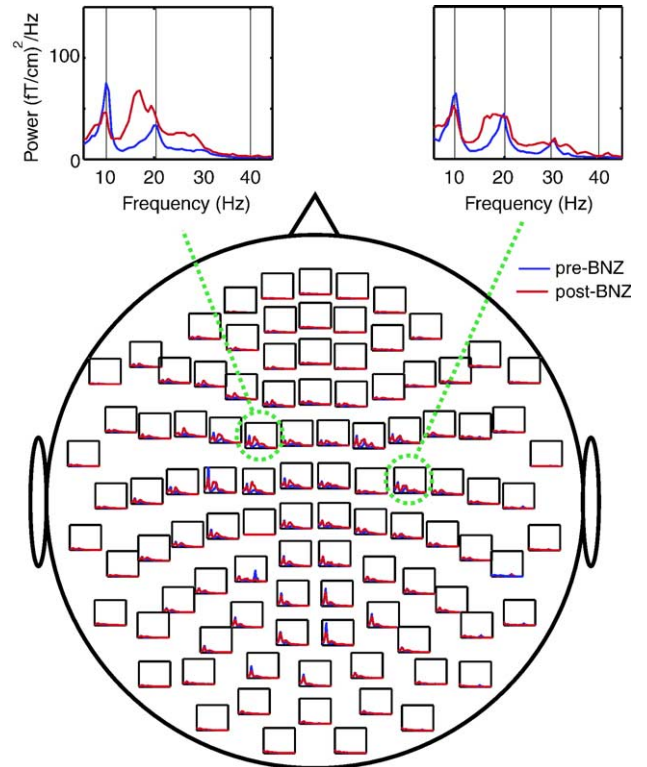


Fig. 1. The power spectra for subject S2 calculated for the spontaneous brain activity measured before (pre-BNZ, blue lines) and after (post-BNZ, red lines) the application of benzodiazepine. The spectra are arranged according to the sensor locations on the helmet; spectra from planar gradiometers with the same location but orthogonal orientations are averaged.

The spectra are arranged according to sensor locations on the helmet. Each spectrum is the average calculated from two orthogonal planar gradiometers at the same position. The enlarged graphs show the spectra from a set of gradiometers over the sensorimotor cortex. In the pre-BNZ condition, the rolandic mu rhythm consists of  $\approx 10$  Hz and  $\approx 20$  Hz main frequencies. In the post-BNZ condition, the  $\approx 10$  Hz peak is weaker, whereas the  $\approx 20$  Hz peak is now stronger and broader than during pre-BNZ, extending towards lower frequencies.

To estimate the brain regions generating the changes in the 10 and 20 Hz bands sensitive to benzodiazepine, we first calculated the increase in power for the planar gradiometers. Fig. 2 shows the grand average of the Z-transformed power values for the pre-BNZ subtracted from the post-BNZ on the geometry of the sensor helmet. No significant changes were observed in the 9–13 Hz band (Fig. 2a). A highly significant increase was observed in the 13–35 Hz band in sensors over the primary sensorimotor cortices of both hemispheres (Fig. 2b).

To more accurately pinpoint the neuronal generators of alpha and beta oscillations sensitive to benzodiazepine, we calculated the minimum current estimates (MCEs) in the frequency domain for individual subjects at the frequency of the strongest alpha and beta peaks (Jensen and Vanni, 2002) (the beta frequency values indicated in Fig. 4b). Fig. 3 shows the grand average MCEs for the 8 subjects (in one subject, we did not have the MRI and applied a standard brain model instead when determining the head model). The strongest sources accounting for the activity in the 10 Hz band

were identified in the left and right primary sensorimotor areas and the parieto-occipital sulcus. The activity in the alpha band changed little with the application of benzodiazepine. The sources of activity in the beta band were in the sensorimotor cortex bilaterally, and they became stronger after the application of benzodiazepine (Fig. 3b). Note that the locations of the source are consistent with increase in beta power observed at the sensors in Fig. 2. Fig. 3b shows a representative example in which the centers of the sources of the beta activity were coregistered with the subject's MRI. The source location agrees with hand sensorimotor cortex in the central sulcus. The locations of the sources before (blue red lines) and after (red lines) benzodiazepine administration are virtually indistinguishable.

To quantify the effect of benzodiazepine, we selected 18 gradiometers over the left and 18 over the right sensorimotor cortex, as indicated in Fig. 4a. The power spectra were then averaged over both hemispheres for this set of gradiometers for each subject. The individual frequencies in the 13–35 Hz band were identified as the spectral peaks. The peaks and the corresponding values are indicated in Fig. 4b. In two subjects (S3 and S4), no clear frequency peaks were identified in the pre-BNZ condition, however, there was an indication of the beta rhythm observed as a “shoulder” in the power spectra. Interestingly, in both subjects, a peak emerged in the post-BNZ condition. In the remaining 6 subjects, beta frequencies were decreased by an average value of 1.6 Hz ( $P < 0.033$ ; paired  $t$  test, 2-tailed).

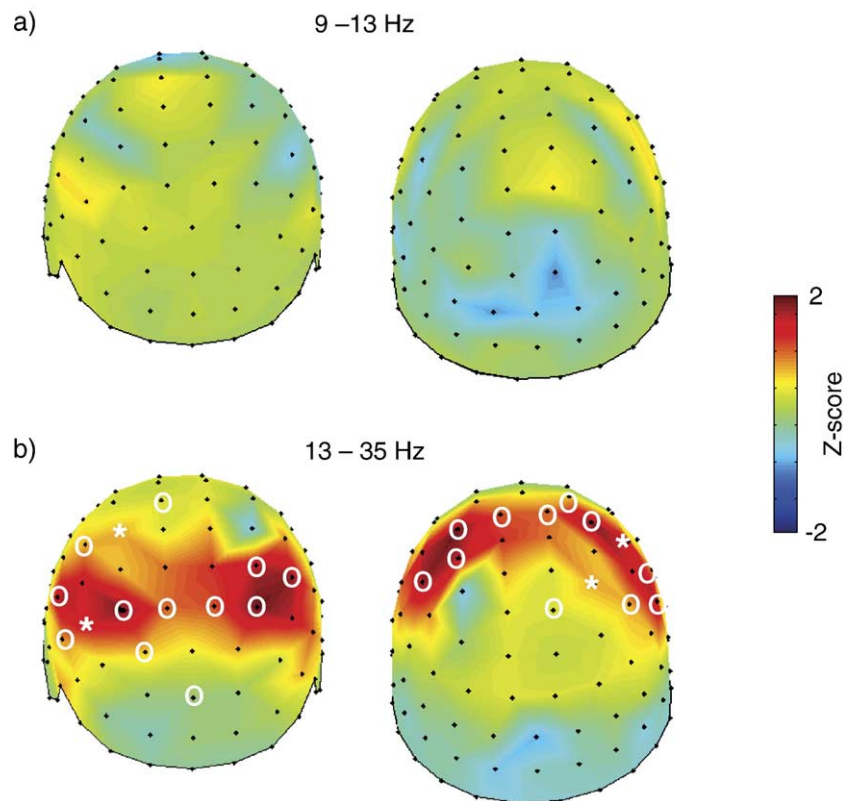


Fig. 2. The difference in (a) alpha power and (b) beta power between the benzodiazepine and control condition represented on the geometry of the helmet (shown from top-front and back). The color code represents the grand average of the Z-transformed power for the 8 subjects. The \*'s denote sensor locations where both of the two orthogonal planar gradiometers with the same position had a significant increase ( $P < 0.01$ ) and o's sensor locations where one of the two gradiometers had a significant increase.

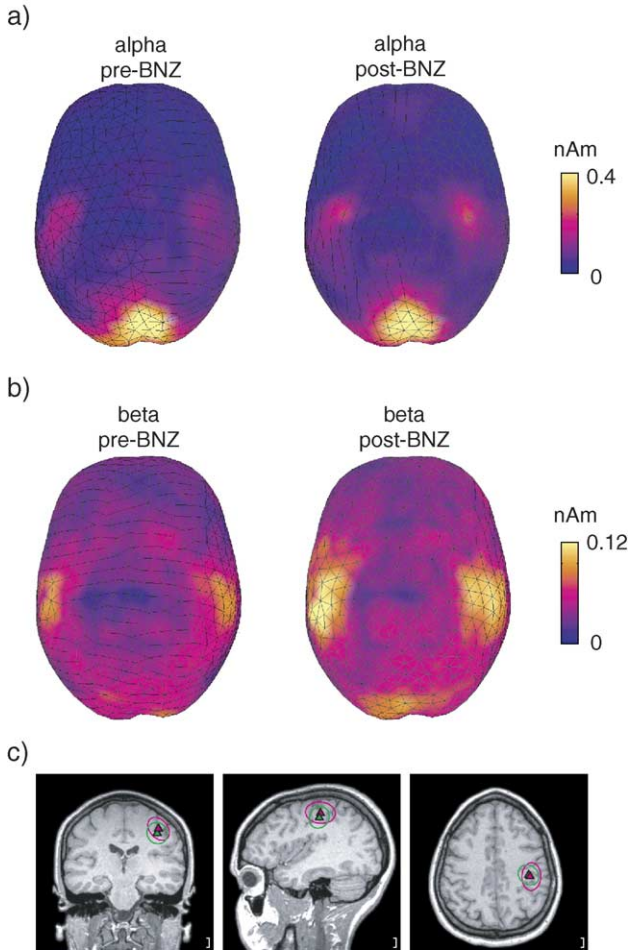


Fig. 3. The grand average of the minimum currents estimates of spontaneous oscillatory projected to the brain surface before and after the application of benzodiazepines. (a) Sources accounting for activity in the 8–12 Hz band were strongest in primary sensorimotor areas (left and right) and around to the parietal-occipital sulcus. (b) Sources in the 13–35 Hz band were found in primary sensorimotor areas with an increase after application of the benzodiazepine. (c) A representative example showing that co-registration of the center of the beta band sources on S2’s MRI. The centers before and after application of benzodiazepines are virtually identical (pre-BNZ, green symbols; post-BNZ, red symbols).

Modeling

The aim of the modeling was to show that there is a physiologically reasonable parameter range in which an increase in  $GAB_A$ -mediated conductance can increase the power in the beta-frequency band, broaden the spectrum and decrease the frequency, as in the data presented above. Since the power in the alpha-frequency band was relatively unaltered by benzodiazepine and since it has been argued that alpha and beta oscillations have different generators (Hari and Salmelin, 1997), the modeling did not aim to account for oscillatory activity in the alpha band. The network (Fig. 5a) contains excitatory (e) and inhibitory (i) cells, each modeled by Hodgkin–Huxley dynamics (see Materials and methods), with connections from i-cells to e-cells and to other i-cells and connections from e-cells to i-cells. There are also recurrent excitatory connections, but these are very small and do not affect the dynamics of the network; however, they are the

source of the model MEG signal that we present. We cannot exclude that thalamo-cortical connections are important for modulating the beta rhythm as well; however, in this work, we assume that a neocortical network alone is responsible for producing the beta rhythm (see Materials and methods for details and discussion on the modeling of the MEG signal).

The  $GAB_A$  decay time was chosen to be at  $\tau_i$  12 ms. The other parameters of the baseline dynamics shown here were chosen so that the frequency of the rhythm is in the beta-range and dependent primarily on tonic AMPA-mediated input. Fig. 5b shows an example from the simulations in which the voltage trace of 5 of the 64 e-cells and three of the 16 i-cells are shown. The i-cells fire spikes (action potentials) synchronously at  $\approx 20$  Hz. The sparse firing of the e-cells is locked to the rhythm determined by the i-cells.

Fig. 6a shows the computed power spectra, mainly reflecting the firing of the e-cells, for three values of the inhibitory conductance between i-cells ( $g_{ii}$ ). As the conductance is increased, the power in the beta frequency range increases, the maximal power increases, and the spectral peak widens. Furthermore, the frequency decreases.

Fig. 6b shows the power spectra for increasing values of  $g_{ie}$ , the maximal inhibitory conductance for the e-cells. Note that, as  $g_{ie}$  increases, the power decreases, the frequency remains constant, and the spectral peak becomes thinner.

The mechanism behind the above results can be understood from the raster plots in which the time of firing of each cell is illustrated as dots as shown in Figs. 7 and 8. The firing times of the i- and e-cells are plotted as respectively the lower and upper

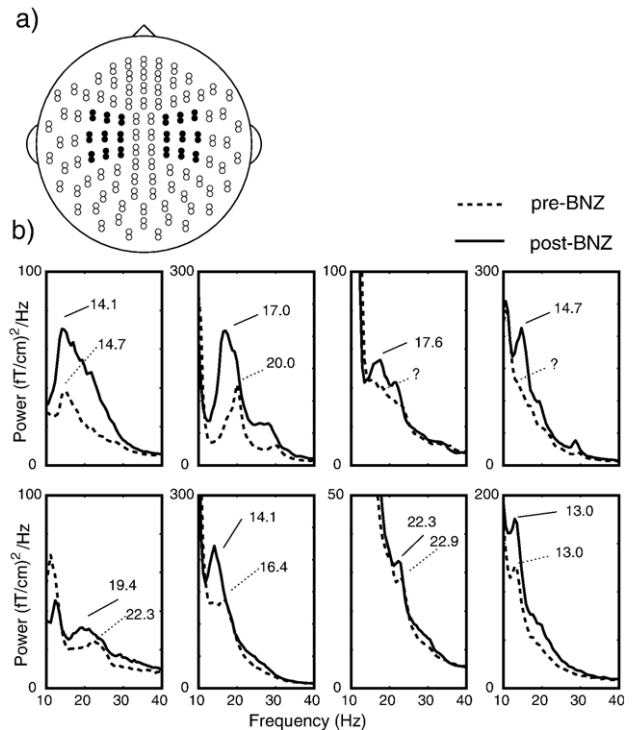


Fig. 4. The black dots in panel (a) mark the planar gradiometers over sensorimotor areas used to calculate the averaged spectra in panel (b). The dotted and solid lines indicate the spectra for all 8 subjects calculated for the condition respectively without and with benzodiazepines. The numerical values refer to the identified peaks in the beta band.

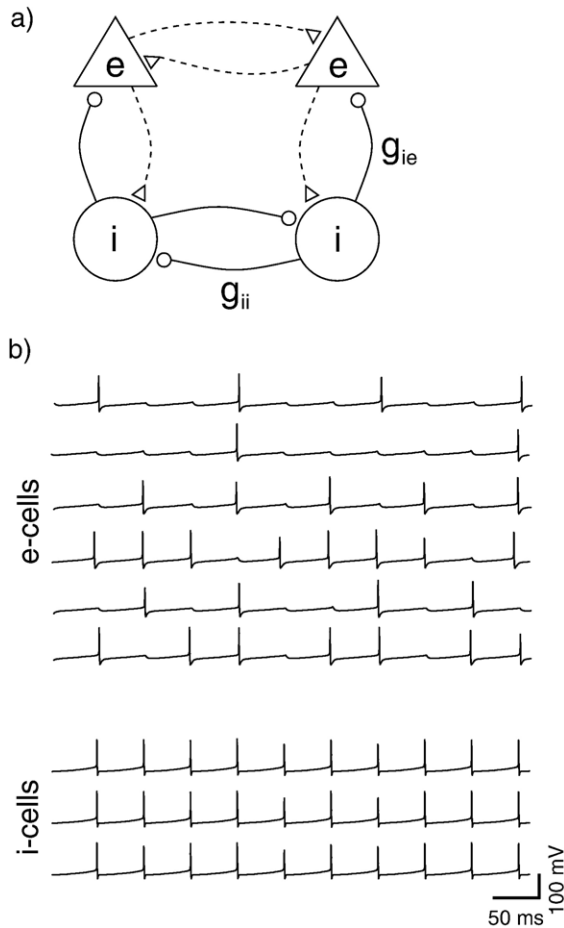


Fig. 5. (a) A schematic diagram of the model constructed of 64 excitatory (e-cells) and 16 inhibitory (i-cells) cells. In the simulations, we investigated the consequences of changing the inhibitory conductances to respectively inhibitory ( $g_{ii}$ ) and excitatory ( $g_{ie}$ ) cells. (b) A simulation example showing the membrane potentials of a subset of e- and i-cells where  $GABA_A$  conductances were  $g_{ii} = 7 \text{ mS/cm}^2$  and  $g_{ie} = 0.9 \text{ mS/cm}^2$ .

portion and then ordered according to the amount of external drive. The key point is that, since the e-cells have a range of external drives, only cells that have enough drive will spike before the next pulse of inhibition.

Fig. 6a shows that when  $g_{ii}$  is increased, the period of the underlying rhythm increases. The raster plots of Figs. 7a–c show that the increase of the period allows more e-cells to fire in a given period. The firing of e-cells for larger values of  $g_{ii}$  is more spread out within a given cycle. This is seen in Fig. 7d where the histograms of the phase of firing of the e-cells are shown relative to the firing of the i-cells. As the time window in which the e-cells can fire is broadening with  $g_{ii}$ , more e-cells become involved in the rhythm thereby resulting in increased power. This is true because the e-cells fire when the inhibition has decayed sufficiently, depending on the drive to those cells (Borgers and Kopell, 2003; Ermentrout and Kopell, 1998). As the period increases and the inhibition to the e-cells is not changing, there is a longer interval for the e-cells to fire before the next bout of inhibition. The set of e-cells that are allowed to fire in a given cycle can be derived analytically (not shown).

Increasing  $g_{ie}$  has a different effect, as is shown in Fig. 8: the e-cells receive more inhibition, and fewer cells fire. However, as

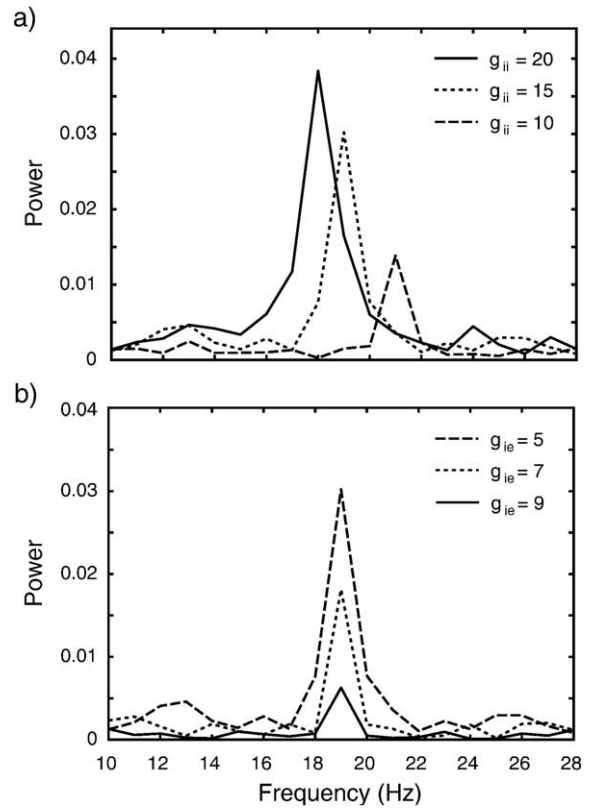


Fig. 6. Power spectra of the quantity  $EPSC_{tot}$  defined by Eq. (1) for different values of the inhibitory conductance. (a) The power increases as  $g_{ii}$  is increased from 10 to 20  $\text{mS/cm}^2$  and  $g_{ie}$  is constant at 5  $\text{mS/cm}^2$ . (b) The power decreases as  $g_{ie}$  is increased from 5 to 9  $\text{mS/cm}^2$  and  $g_{ii}$  is constant at 15  $\text{mS/cm}^2$ .

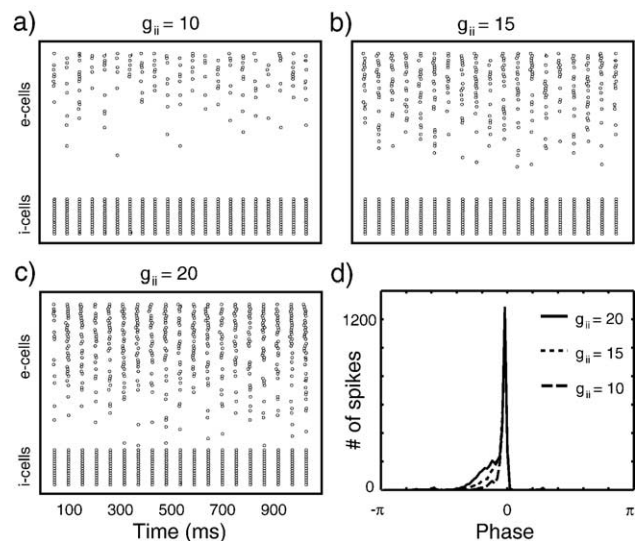


Fig. 7. Raster plots of the excitatory and inhibitory neurons in the network. (a–c) The upper portion shows the firing times of the e-cells ordered by the amount of drive applied to each of them with the cells in the highest row receiving the largest drive. Lower portion shows the spike times of the i-cells. In all plots,  $g_{ie} = 5 \text{ mS/cm}^2$ ;  $g_{ii}$  takes on values of 10, 15 and 20  $\text{mS/cm}^2$  in the successive plots. Panel (d) shows a histogram of the phases of spike times over a run of 100 periods with respect to the firing of the i-cells for the three rasters in panels (a–c).

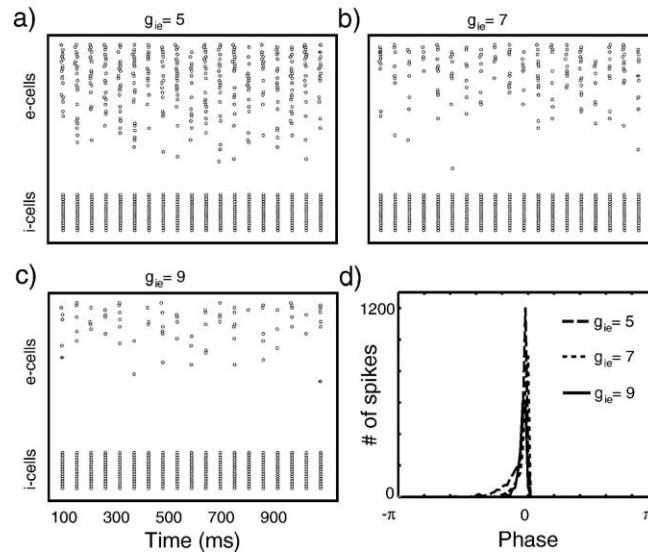


Fig. 8. Similar to Fig. 7, but here  $g_{ii} = 15 \text{ mS/cm}^2$  is fixed and  $g_{ie}$  takes on values 5, 7 and 9  $\text{mS/cm}^2$ .

shown both in the power spectra (Fig. 6b) and the histogram (Fig. 8d), the active e-cells fire more coherently. The reason is the converse of the decrease in coherence for increasing  $g_{ii}$ : As  $g_{ie}$  increases, the inhibition to the e-cells suppresses the firing of the latter for a longer proportion of the period, and hence those that fire must do so more coherently. In other words: the time window in which the e-cells can fire becomes shorter as  $g_{ie}$  increases since  $g_{ie}$  is preventing the firing. In these simulations, the coupling from the e-cells to the i-cells,  $g_{ei}$ , was chosen to be small. A somewhat larger value of  $g_{ei}$  did not appreciably change the results (data not shown).

## Discussion

Using magnetoencephalographic recordings in humans, we observed a strong increase with benzodiazepines in the power of beta oscillations in the primary sensorimotor regions of both hemispheres. The increase in power was associated with a small decrease in the beta frequency. The beta oscillations sensitive to benzodiazepine originated from the primary sensorimotor cortex, close to the hand area. Ours is the first study to demonstrate that the 20-Hz oscillations emerging after benzodiazepine also originate from the sensorimotor cortex and that the oscillations decrease in frequency with benzodiazepine. Previous work has identified sources of beta-range activity in the primary motor cortex (reviewed in Hari and Salmelin, 1997). In these studies, the beta activity was observed during rest or was induced 300–1000 ms after somatosensory stimulation or movement. Using intracranial recordings, beta oscillations have also been observed in the motor cortex of monkeys (Baker et al., 1997; Jackson et al., 2002; Murthy and Fetz, 1996; Sanes and Donoghue, 1993). Our findings strongly suggest that it is these motor-cortex beta sources which are modulated by benzodiazepine. We therefore conclude that the motor cortex is a primary cortical effector site of benzodiazepine. This is consistent with benzodiazepines acting as muscle relaxants. Our results are at first sight at odds with scalp EEG recordings which show that beta power primarily increases over frontal regions after application of benzodiazepines

(Wanquier, 1998). However, tangential current dipoles in the wall of the central sulcus can produce strong electrical potentials over frontal areas. At the same time, the planar gradiometers used in the present study measure the strongest magnetic signal over the sensorimotor areas.

The primary effect of benzodiazepine is to increase the conductance of  $GAB_A$ -mediated currents. Computer simulations of a network of biophysically-based model neurons could account for the increase in the power of the beta oscillations by an increase in synaptic conductance of  $GAB_A$ -mediated inhibition. As in the experiments, the increase in power was associated with a decrease in frequency and a widening of the spectral peak. An increase in the GABAergic inhibition among i-cells was sufficient to produce these effects, while an increase in inhibition to e-cells alone was not sufficient. Even though we argue that the main effect of benzodiazepine is on the network of i-cells, the i-cells strongly modulate the firing of pyramidal e-cells. The resulting changes in excitatory post-synaptic currents in the dendrites of the pyramidal e-cells likely result in the signals detected by MEG.

The above results do not imply that the network produces beta-band oscillations only through the interactions of i-cells. However, based on extensive simulations (data not shown), we will argue that an interneuron based beta (INB) mechanism reproduces the spectral results much better than a rhythm based on the interaction between pyramidal and inhibitory neurons (PINB). Suppose there is significant excitatory phasic input to the i-cells from the e-cells and significant phasic inhibition to the e-cells. The i-cells then fire only during the peaks of the e-cell output. We aim to slow the rhythm down by increasing the i–i conductance. With i-cells spiking less frequently, the inhibition to the e-cells is decreased, allowing more of the latter to fire; this, in turn speeds up the i-cells if the  $e \rightarrow i$  coupling is strong. Thus, in a PINB regime, in which the i-cells are significantly affected by e-cell firing, frequency is not responsive to changing the i–i conductance. As a consequence, the change in power with a change in i–i conductance will also be modest and cannot account for the experimental results. The frequency is strongly affected by the strength of the  $i \rightarrow e$  connections. However, increasing  $i \rightarrow e$  connections alone makes

the power decrease, since fewer e-cells fire. Increase of inhibition to e-cells also narrows the window within which e-cells can fire; this makes the e-cells more synchronous and the spectral band narrower, instead of the observed broadening.

In contrast, the INB mechanism (Figs. 7 and 8) is very sensitive to the *i*–*i* conductance since the main driving force is tonic. Thus, the period of the *i*-cells is determined not by when the e-cells fire, but rather when the *i*–*i* inhibition wears away. The strong *i* → e connections then act as a gate allowing e-cells to fire only at certain intervals. The main role of AMPA receptors on the *i*-cells in this model is to create a tonic drive to the *i*-cells. The prediction that the interneuronal network is responsible for producing the motor cortical beta rhythm can be tested in *in vitro* slice preparations. Specifically, we predict that beta oscillations can be produced in motor cortical slice preparations following application of an AMPA antagonist given that the interneurons are sufficiently depolarized pharmacologically.

Hippocampal *in vitro* slices have been shown to produce gamma and beta frequency rhythms with a spontaneous transition between them (Whittington et al., 1997b). The spontaneous switch was modeled in large networks by Traub et al. (1999) and explained in a simpler model by Kopell et al. (2000). This model was subjected to further analysis that investigated the transition between the gamma and beta states (Sosnovtseva et al., 2002). However, the mechanism in this model does not produce the beta rhythm when the excitatory cells of the network fire sparsely, as is the case in the sensory and motor cortices when no tasks are performed (e.g. Mushiake et al., 1991). Another study on the effects of benzodiazepines on rhythms (*in vitro* gamma and beta rhythms) was done on hippocampal rat slices (Faulkner et al., 1999) and did not show the same effects we are reporting here. Another rat hippocampal slice study on cholinergically induced beta oscillations demonstrated a clear increase in the power of beta oscillations as well as a decrease in frequency with benzodiazepine (Shimono et al., 2000).

Even though our study has concentrated on the beta rhythm, other studies have identified changes with benzodiazepines in other frequency bands as well. Fingelkurts et al. (2004) applied both EEG and MEG to study the effect of the lorazepam. Classifying short-term spectral changes, they showed that lorazepam changed the temporal structures of oscillations in the delta, theta and alpha band; however, the specificity of the effects to lorazepam remains to be shown.

The functional role of the motor-cortex beta rhythm remains unclear. The beta rhythm we investigated was observed during rest, and it is not obvious how it is related to beta oscillations present during motor tasks. For instance, the strong synchronization in the beta band between motor cortex and the population firing of motor units in isometrically contracted muscles suggests that the beta rhythm is important for corticomuscle communication (Farmer, 1998; Hari and Salenius, 1999; Kilner et al., 2000; Mima and Hallett, 1999; Salenius and Hari, 2003). Interestingly, Baker and Baker (2003) reported a decrease in corticomuscular coherence in the beta band with benzodiazepines, which might suggest that the beta rhythm we observe during rest is different from the beta rhythm involved in corticomuscular synchronization. However, it should be noted that a change in coherence does not necessarily imply a change in power of the sources involved. Furthermore, Baker and Baker (2003) applied EEG which is more sensitive to convexial cortex whereas MEG picks up signals mainly from the fissural cortex.

Similar dissociation between beta-range rhythms is seen in patients with progressive myoclonus epilepsy who may even have 2–4 times stronger corticomuscular coherence than healthy control subjects although the reactivity of their motor-cortex rhythms to external stimuli suggests reduced cortical inhibition (Silen et al., 2000). Although the increased cortex-muscle coherence could reflect enhanced recalibration of the inaccurate muscle contractions, the question about several functionally distinct beta-range motor-cortex rhythms seems difficult to be resolved without further studies involving pharmacological interventions.

## Acknowledgments

The experimental part of the study has been financially supported by the Academy of Finland, the NWO Innovative Research Incentive Schemes with financial aid from the Netherlands Organization for Scientific Research (NWO) and by the EU's Large-Scale Facility Neuro-BIRCH III hosted at the Brain Research Unit of the Low Temperature Laboratory, Helsinki University of Technology. The theoretical parts of the study have been supported by the National Institute of Health, National Science Foundation and the National Institute of Mental Health, USA. We are grateful to Roger D. Traub for insightful comments and Kimmo Uutela for help on the MCE software.

## References

- Bacci, A., Rudolph, U., Huguenard, J.R., Prince, D.A., 2003. Major differences in inhibitory synaptic transmission onto two neocortical interneuron subclasses. *J. Neurosci.* 23, 9664–9974.
- Baker, M.R., Baker, S.N., 2003. The effect of diazepam on motor cortical oscillations and corticomuscular coherence studied in man. *J. Physiol.* 546, 931–942.
- Baker, S.N., Olivier, E., Lemon, R.N., 1997. Coherent oscillations in monkey motor cortex and hand muscle EMG show task-dependent modulation. *J. Physiol.* 501 (Pt. 1), 225–241.
- Borgers, C., Kopell, N., 2003. Synchronization in networks of excitatory and inhibitory neurons with sparse, random connectivity. *Neural Comput.* 15, 509–538.
- Conway, B.A., Halliday, D.M., Farmer, S.F., Shahani, U., Maas, P., Weir, A.I., Rosenberg, J.R., 1995. Synchronization between motor cortex and spinal motoneuronal pool during the performance of a maintained motor task in man. *J. Physiol.* 489 (Pt. 3), 917–924.
- Ermentrout, G.B., Kopell, N., 1998. Fine structure of neural spiking and synchronization in the presence of conduction delays. *Proc. Natl. Acad. Sci. U. S. A.* 95, 1259–1264.
- Farmer, S.F., 1998. Rhythmicity, synchronization and binding in human and primate motor systems. *J. Physiol.* 509 (Pt. 1), 3–14.
- Faulkner, H.J., Traub, R.D., Whittington, M.A., 1999. Anaesthetic/amnesic agents disrupt beta frequency oscillations associated with potentiation of excitatory synaptic potentials in the rat hippocampal slice. *Br. J. Pharmacol.* 128, 1813–1825.
- Fingelkurts, A.A., Fingelkurts, A.A., Kivisaari, R., Pekkonen, E., Ilmoniemi, R., Kahkonen, S., 2004. The interplay of lorazepam-induced brain oscillations: microstructural electromagnetic study. *Clin. Neurophysiol.* 115, 674–690.
- Hämäläinen, M., Hari, R., Ilmoniemi, R.J., Knuutila, J., Lounasmaa, O.V., 1993. Magnetoencephalography—theory, instrumentation, and applications to noninvasive studies of the working human brain. *Rev. Mod. Phys.* 65, 413–497.
- Hari, R., Salenius, S., 1999. Rhythmical corticomotor communication. *NeuroReport* 10, R1–R10.

- Hari, R., Salmelin, R., 1997. Human cortical oscillations: a neuromagnetic view through the skull. *Trends Neurosci.* 20, 44–49.
- Jackson, A., Spinks, R.L., Freeman, T.C., Wolpert, D.M., Lemon, R.N., 2002. Rhythm generation in monkey motor cortex explored using pyramidal tract stimulation. *J. Physiol.* 541, 685–699.
- Jensen, O., Pohja, M., Goel, P., Ermentrout, B., Kopell, N., Hari, R., 2002. On the physiological basis of the 15–30 Hz motor-cortex rhythm. In: Nowak, H., Haueisen, J., Giessler, F., Huonkier, R. (Eds.), *Proceedings of the 13th International Conference on Biomagnetism*. VDE Verlag GMBH, Berlin, pp. 313–315.
- Jensen, O., Vanni, S., 2002. New method to identify multiple sources of oscillatory activity from magnetoencephalographic data. *NeuroImage* 15, 568–574.
- Juottonen, K., Gockel, M., Silen, T., Hurri, H., Hari, R., Forss, N., 2002. Altered central sensorimotor processing in patients with complex regional pain syndrome. *Pain* 98, 315–323.
- Kilner, J.M., Baker, S.N., Salenius, S., Hari, R., Lemon, R.N., 2000. Human cortical muscle coherence is directly related to specific motor parameters. *J. Neurosci.* 20, 8838–8845.
- Kilner, J.M., Baker, S.N., Salenius, S., Jousmäki, V., Hari, R., Lemon, R.N., 1999. Task-dependent modulation of 15–30 Hz coherence between rectified EMGs from human hand and forearm muscles. *J. Physiol.* 516 (Pt. 2), 559–570.
- Kopell, N., Ermentrout, G.B., Whittington, M.A., Traub, R.D., 2000. Gamma rhythms and beta rhythms have different synchronization properties. *Proc. Natl. Acad. Sci. U. S. A.* 97, 1867–1872.
- Mima, T., Hallett, M., 1999. Corticomuscular coherence: a review. *J. Clin. Neurophysiol.* 16, 501–511.
- Murthy, V.N., Fetz, E.E., 1996. Oscillatory activity in sensorimotor cortex of awake monkeys: synchronization of local field potentials and relation to behavior. *J. Neurophysiol.* 76, 3949–3967.
- Mushiake, H., Inase, M., Tanji, J., 1991. Neuronal activity in the primate premotor, supplementary, and precentral motor cortex during visually guided and internally determined sequential movements. *J. Neurophysiol.* 66, 705–718.
- Press, W.H., Teukolsky, S.A., Vetterling, W.T., Flannery, B.P., 1997. *Numerical Recipes in C*. Cambridge Univ. Press, USA.
- Salenius, S., Hari, R., 2003. Synchronous cortical oscillatory activity during motor action. *Curr. Opin. Neurobiol.* 13, 678–684.
- Salenius, S., Portin, K., Kajola, M., Salmelin, R., Hari, R., 1997. Cortical control of human motoneuron firing during isometric contraction. *J. Neurophysiol.* 77, 3401–3405.
- Sanes, J.N., Donoghue, J.P., 1993. Oscillations in local field potentials of the primate motor cortex during voluntary movement. *Proc. Natl. Acad. Sci. U. S. A.* 90, 4470–4474.
- Shimono, K., Brucher, F., Granger, R., Lynch, G., Taketani, M., 2000. Origins and distribution of cholinergically induced beta rhythms in hippocampal slices. *J. Neurosci.* 20, 8462–8473.
- Silen, T., Forss, N., Jensen, O., Hari, R., 2000. Abnormal reactivity of the approximately 20-Hz motor cortex rhythm in Unverricht Lundborg type progressive myoclonus epilepsy. *NeuroImage* 12, 707–712.
- Sosnovtseva, O.V., Setsinsky, D., Fausboll, A., Mosekilde, E., 2002. Transitions between beta and gamma rhythms in neural systems. *Phys. Rev. E Stat. Nonlin. Soft Matter Phys.* 66, 041901–1.
- Towers, S.K., LeBeau, F.E., Gloveli, T., Traub, R.D., Whittington, M.A., Buhl, E.H., 2002. Fast network oscillations in the rat dentate gyrus in vitro. *J. Neurophysiol.* 87, 1165–1168.
- Traub, R.D., Miles, R., 1991. *Neuronal Networks of the Hippocampus*. Cambridge Univ. Press.
- Traub, R.D., Whittington, M.A., Buhl, E.H., Jefferys, J.G., Faulkner, H.J., 1999. On the mechanism of the gamma → beta frequency shift in neuronal oscillations induced in rat hippocampal slices by tetanic stimulation. *J. Neurosci.* 19, 1088–1105.
- Traub, R.D., Whittington, M.A., Colling, S.B., Buzsáki, G., Jefferys, J.G., 1996. Analysis of gamma rhythms in the rat hippocampus in vitro and in vivo. *J. Physiol. (Lond.)* 493, 471–484.
- Uutela, K., Hamalainen, M., Somersalo, E., 1999. Visualization of magnetoencephalographic data using minimum current estimates. *NeuroImage* 10, 173–180.
- Wanquier, A., 1998. EEG and neuropharmacology, in electroencephalography. In: Niedermeyer, E., Lopes da Silva, F. (Eds.), *Basic Principles, Clinical Applications, and Related Fields*. Williams and Wilkins, pp. 660–670.
- Whittington, M.A., Traub, R.D., Jefferys, J.G., 1995. Synchronized oscillations in interneuron networks driven by metabotropic glutamate receptor activation. *Nature* 373, 612–615.
- Whittington, M.A., Stanford, I.M., Colling, S.B., Jefferys, J.G., Traub, R.D., 1997a. Spatiotemporal patterns of gamma frequency oscillations tetanically induced in the rat hippocampal slice. *J. Physiol.* 502 (Pt. 3), 591–607.
- Whittington, M.A., Traub, R.D., Faulkner, H.J., Stanford, I.M., Jefferys, J.G., 1997b. Recurrent excitatory postsynaptic potentials induced by synchronized fast cortical oscillations. *Proc. Natl. Acad. Sci. U. S. A.* 94, 12198–12203.